Electronic Structure and Chemical Bonding in the Lowest Electronic States of TcN†

Antonio Carlos Borin* and João Paulo Gobbo

Instituto de Química, Universidade de São Paulo Av. Prof. Lineu Prestes, 748. 05508-900 São Paulo, SP, Brazil

Received: March 20, 2009; Revised Manuscript Received: May 13, 2009

Multiconfiguration second-order perturbation theory, with the inclusion of relativistic effects and spin−orbit coupling, was employed to investigate the nature of the ground and low-lying Λ−S and Ω states of the TcN molecule. Spectroscopic constants, effective bond order, and potential energy curves for 13 low-lying Λ−S states and 5 Ω states are given. The computed ground state of TcN is of Ω = 3 symmetry (R_e = 1.605 Å and ω_e = 1085 cm^{-1}), originating mainly from the $^3\Delta$ Λ−S ground state. This result is contrasted with the nature of the ground state for other VIIB transtion-metal mononitrides, including $X^3\Sigma^-$ symmetry for MnN and Ω = 0^+ symmetry for ReN, derived also from a $X^3\Sigma^-$ state.

1. Introduction

Chemical compounds formed by combining transition metals and main group elements are important not only from a technological point of view but also from a more fundamental perspective.[1] For instance, understanding the nature of the chemical bonding between nitrogen and transition metals is fundamental for understanding nitrogen fixation in both biological and industrial processes. Because of the electronic characteristics of the transition metals that encompass several low-lying electronic states in a very narrow energy range, a great variety of chemical bonding and molecular states can be obtained after combining them with other chemical elements.

Diatomic transition-metal nitrides have received attention because of special electronic and magnetic properties, with possible applications in spintronics.[2−5] Very important aspects related to the metal−nitrogen chemical bonding can be better understood after a careful analysis of the corresponding diatomic species, a fundamental step toward the comprehension of the physical chemical properties of more complex systems.

The ground states of the VIIB transition-metal atoms are derived from the $(n + 1)s^2nd^5$ electronic configuration, corresponding to ^{6}S states.[6] Therefore, to form a chemical bond, it is necessary to overcome the first atomic excitation energy, $(n + 1)s^2nd^5(^6S) \rightarrow (n + 1)s^1nd^6(^6D)$. For the Mn atom, this amounts to 2.14 eV (*J*-averaged value), whereas for Tc (0.41 eV) and Re (1.71 eV) atoms, much less energy is necessary (experimental values in parentheses).[6] Andrews et al.[7] employed laser vaporization technique, infrared spectroscopy, and density functional theory (DFT) to investigate the MnN species, reporting a ground state of $^5\Pi$ symmetry almost degenerate with a $^3\Sigma^-$ electronic state (T_e = 0.03 eV). ReN was investigated by Balfour et al.,[8,9] who concluded, on the basis of laser-induced and dispersed fluorescence experimental results, that the ground state is a $X^3\Sigma^-$ (Ω = 0^+) state with the other component (Ω = 1) 2630 cm^{-1} higher in energy. They have also reported spectroscopic constants for a $^3\Delta$ electronic state, with corresponding values for the Ω = 1, 2, and 3 components.

A few diatomic compounds formed between technetium and main group elements are known. Jackson et al.[10] employed experimental (electron ionization−Knudsen mass electronic spectra) and computational (DFT) methods to determine the dissociation energy of TcC. At the DFT level (B3LYP functional), the ground state was computed to be a $^4\Sigma^-$ state (electronic configuration $10\sigma^2 11\sigma^2 5\pi^4 12\sigma^1 2\delta^2$, R_e = 1.710 Å, ω_e = 937 cm^{-1}) with a dissociation energy (D_0 = 6.94 eV) in agreement with the experimental value (D_0 = 6.02 ± 0.1 eV). TcO and TcS were investigated theoretically by Langhoff et al.[11] at the modified coupled pair functional level (MCPF) of theory, with the inclusion of relativistic corrections. The ground state of TcO was computed to be a $^6\Sigma^+$ state (R_e = 1.772 Å, ω_e = 795 cm^{-1}, and D_0 = 3.55 eV), whereas a $^6\Sigma^+$ state (R_e = 2.168 Å, ω_e = 492 cm^{-1}, and D_0 = 2.91 eV) was reported for TcS. To the best of our knowledge, there is no information about technetium mononitride.

In the last years, we have embarked on a project for describing electronic and spectroscopic properties of diatomic compounds involving transition metals, with either metal−metal bonding or metal−main-group-element chemical bonding. In transition-metal atoms, the nd orbitals are partially occupied, and the corresponding electrons are tightly packed, giving rise to a high density of low-lying atomic states that are able to form a multitude of chemical bonds with strong dynamic correlation effects.[12−14] Therefore, to obtain a good description of properties of compounds containing transition metals, it is necessary to employ multiconfigurational methods that can recover both static and dynamic electron correlation effects. The multiconfigurational second-order perturbation theory (CASPT2), based on a complete active space self-consistent field (CASSCF) wave function,[15−18] has proved to be accurate for describing the chemical bonding as well as other relevant physical chemical properties of variety of diatomic species containing transition metals such as CoC,[19] RhB,[20,21] Mo_2,[22] Tc_2, and Re_2.[23]

To contribute to a better understanding of the chemical bonding and electronic spectroscopic properties of diatomic species between transition metals and main group elements, we have carried out a detailed study of the TcN species at the CASSCF/CASPT2 level, reporting potential energy curves, spectroscopic constants, and relevant aspects of the nature of the chemical bonding for several low-lying electronic states.

† Part of the "Russell M. Pitzer Festschrift".

* Corresponding author. E-mail: ancborin@iq.usp.br. Fax: +55-11-3815 5579. Tel: +55-11-3091 3073.

10.1021/jp902545h CCC: $40.75
Published on Web 06/11/2009

TABLE 1: Low-Lying Λ−S Electronic States of TcN, Their Dissociation Channels, and Energy Separation at the Dissociation Limit

		excitation energy (cm^{-1})	
state of separated atoms	molecular states	experimental[a]	theoretical
$Tc(^6S) + N(^4S°)$	$^{3,5,7,9}\Sigma^-$	0	0
$Tc(^6D) + N(^4S°)$	$^{3,5,7,9}\{\Sigma^-, \Pi, \Delta\}$	3576	3000

[a] *J*-averaged values from ref 6.

2. Methodology

The lowest-lying Λ−S electronic states of TcN were investigated at the CASSCF/CASPT2 level of theory, including scalar relativistic corrections with the Douglas−Kroll−Hess (DKH) approximation;[24,25] quadruple-ζ ANO-RCC[26,27] atomic basis sets were used for describing the atomic species (Tc: [21s18p13d6f4g-2h/8s7p5d3f2g1h] and N: [14s9p4d3f2g/5s4p3d2f]). At the CASSCF step, zeroth-order wave functions were generated, including the Tc 4d and 5s orbitals and the N 2s and 2p orbitals in the active space (12 electrons in 10 orbitals). Then, dynamic correlation effects were added at the CASPT2 level, with the new zeroth-order Hamiltonian suggested by Ghigo et al.[28] with a shift parameter of 0.25 hartree. At the CASPT2 step, the Tc 4s and 4p electrons were included in the active space, and the others remained frozen. Intruder states were avoided by the use of an imaginary shift of 0.1 hartree.

Calculations were carried out using the C_2 point group symmetry, with averaging over degenerate pairs of states with the same spin and spatial symmetry. The triplet electronic states belonging to the A irreducible representation (IRREP) ($\Sigma^{\pm}$ and Δ states) were described by averaging over the three lowest-lying states, whereas those belonging to the B IRREP (Π states) were computed by averaging over the lowest four states. The quintets, heptets, and nonets belonging to the A IRREP were computed by averaging over three, one, and two electronic states, respectively; for the B IRREP, the average was carried out over three, four, and one electronic states, respectively.

We included the spin−orbit coupling effects (Ω states) by using an atomic mean field approximation for the two-electron part of the DKH spin−orbit Hamiltonian,[29] as implemented in the RASSI (restricted active space state interaction) approach.[30] The computed Λ−S CASSCF wave functions were used as basis functions, and the diagonal elements of the Hamiltonian were replaced by the corresponding energy values computed at the CASPT2 level, thereby taking into account the dynamic correlation effects.[31]

We obtained potential energy curves by fitting cubic splines to the computed energies, which were used to compute vibrational wave functions and energies by numerical integration of the rovibrational Schrodinger equation, as implemented in the Vibrot[32] software. Spectroscopic constants were determined by least-squares fit to the computed rovibrational levels, and dissociation energies were determined to be the difference between the total energies at the equilibrium internuclear distance and those at the correct dissociation limit (R = 50.0 au). All calculations were carried out with the aid of MOLCAS-6.4 software.[32]

3. Results and Discussion

We focused our attention on the lower 13 Λ−S molecular electronic states (Table 1), which are derived by considering a weak spin−orbit nonrelativistic adiabatic correlation[33] with the first two lowest energy dissociation atomic limits, as predicted by the Wigner−Witmer rules.[33,34] The computed potential energy curves are plotted in Figure 1, and the corresponding spectroscopic constants and effective bond orders (EBOs) are displayed in Table 2.

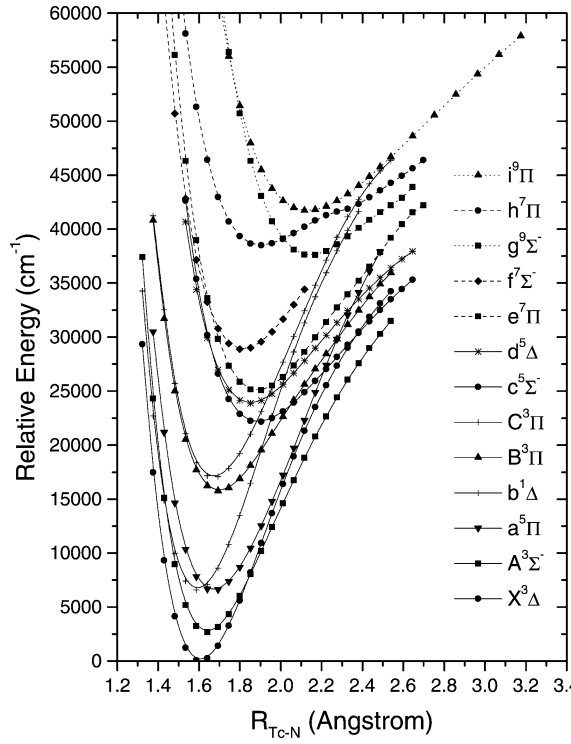

Figure 1. Potential energy curves for the lowest-lying Λ−S states of TcN.

3.1. Ground and Lowest-Lying Electronic States of TcN. Before going into the details of the nature of the ground electronic state of TcN, it is worth commenting on the ground electronic state of the other VIIB transition-metal mononitrides. The first member of the series is the species MnN, for which the DFT studies carried out by Andrews et al.[7] and Wu[35] pointed to a ground state of $^5\Pi$ symmetry (R_e = 1.636 (1.632) Å, ω_e = 706 (704) cm^{-1})[7,35] with D_e = 2.22 eV.[35] At the same level of theory, the authors found that the $^5\Pi$ state would be (T_e) 280 cm^{-1} more stable than the lowest-lying $^3\Sigma^-$ state (R_e = 1.522 Å and ω_e = 820 cm^{-1}).[7] Nonetheless, it is worth keeping in mind that DFT results are very dependent on the functional employed and can fail to predict the correct energetic order of electronic states.[36−38] To have a better description for the ground state of MnN, we decided to perform some test calculations, employing a procedure similar to that described above but with triple-ζ atomic ANO-RCC basis sets[27] for describing the Mn [21s15p10d6f4g2h/6s5p3d2f1g] and N [14s9p4d3f/4s3p2d1f] atoms. Our results indicate that the ground state of MnN is a $X^3\Sigma^-$ state ($|X^3\Sigma^-\rangle = (0.71)|7\sigma^2 8\sigma^2 9\sigma^2 3\pi^4 1\delta^2\rangle$), with an equilibrium internuclear distance (R_e) of 1.631 Å, a dissociation energy (D_e) with respect to the Mn ($^6S(3d^5 4s^2)$) and N ($^4S^o(2s^2 2p^3)$) ground-state atoms of 2.15 eV, a vibrational harmonic frequency (ω_e) of 800 cm^{-1}, and a dipole moment (μ) of 0.99 D ($Mn^{\delta+}N^{\delta-}$). The most important valence molecular orbitals (VMOs) can be described as follows: the 7σ VMO is a nonbonding orbital localized on the nitrogen atom, the 8σ VMO is a bonding orbital formed by the combination of the atomic $2p_z$ N orbital with the M_n $3d_\sigma$, and the 9σ VMO is basically the 4s Mn atomic orbital, that is, a nonbonding orbital. The 1δ VMO is an atomic orbital centered on the Mn atom, corresponding to the $3d_{x^2-y^2}$ and $3d_{xy}$ ($3d_\delta$) orbitals, giving it a

TABLE 2: Theoretical Spectroscopic Constants and Effective Bond Order for the Lowest-Lying Electronic Λ−S States of TcN

electronic state	R_e (Å)	ω_e (cm^{-1})	T_e (cm^{-1})	G_0 (cm^{-1})	$\Delta G_{1/2}$ (cm^{-1})	μ (D)	D_e (eV)	EBO
$X^3\Delta$	1.605	1085	0	542	1075	2.38	5.27	2.74
$A^3\Sigma^-$	1.640	1003	2674	500	990	0.25	4.57	2.68
$a^5\Pi$	1.670	947	6521	473	938	2.77	4.46	2.22
$b^1\Delta$	1.591	1131	6576	564	1122	0.20		2.75
$B^3\Pi$	1.697	854	15753	425	841	2.06		2.21
$C^3\Pi$	1.671	965	16998	482	956	2.02		2.22
$c^5\Sigma^-$	1.888	663	22140	330	653	1.53		1.63
$d^5\Delta$	1.850	710	23880	354	699	2.80		1.68
$e^7\Pi$	1.884	726	25044	362	718	2.40		1.23
$f^7\Sigma^-$	1.815	755	28858	376	745	3.26		1.35
$g^9\Sigma^-$	2.144	630	37570	313	618	0.39		1.00
$h^7\Pi$	1.901	622	38489	296	576	1.44		1.00
$i^9\Pi$	2.130	537	41721	267	530	2.18		1.00

nonbonding character. The 3π VMO is a bonding combination between the $3d_\pi$ ($3d_{xz}$ and $3d_{yz}$ ($3d_\pi$ orbitals)) and $2p_\pi$ ($2p_x$ and $2p_y$) atomic orbitals of the Mn and N atoms, respectively, distorted toward the nitrogen; the 4π VMO is the corresponding counterpart. The $a^5\Pi$ electronic state ($|a^5\Pi\rangle = (0.75)|7\sigma^2 8\sigma^2 9\sigma^1 3\pi^4 4\pi^1 1\delta^2\rangle$), correlating with the Mn ($^6D(3d^6 4s^1)$) and N ($^4S^o(2s^2 2p^3)$) atomic limit 2.1 eV above ground-state atoms, was found 4193 cm^{-1} above the $X^3\Sigma^-$ state, with $R_e = 1.606$ Å, $\omega_e = 855$ cm^{-1}, and $\mu = 2.85$ D ($Mn^{\delta+}N^{\delta-}$). As has been shown for the CoN[37] and ScB[38] diatoms, other theoretical studies at the DFT level resulted in the reverse order.

The other member of the series is ReN. Experimental results by Balfour et al.[8,9] and Steimle et al.[39] indicate a $X^3\Sigma^-$ ($\Omega = 0^+$) ground state, represented by the following electronic configuration: $1\sigma^2 2\sigma^2 1\pi^4 1\delta^2 3\sigma^2$. According to a simple molecular orbital correlation diagram,[39] the nature of the molecular orbitals can be described as follows: 1σ is a nonbonding orbital centered on the N(2s) atom, the 2σ is a bonding combination between the Re(6s) and N($2p_\sigma$), the 1π corresponds to the bonding combination of the Re($5d_\pi$) and N($2p_\pi$), and the 1δ is a nonbonding orbital corresponding to the Re($5d_\delta$) atomic orbital.

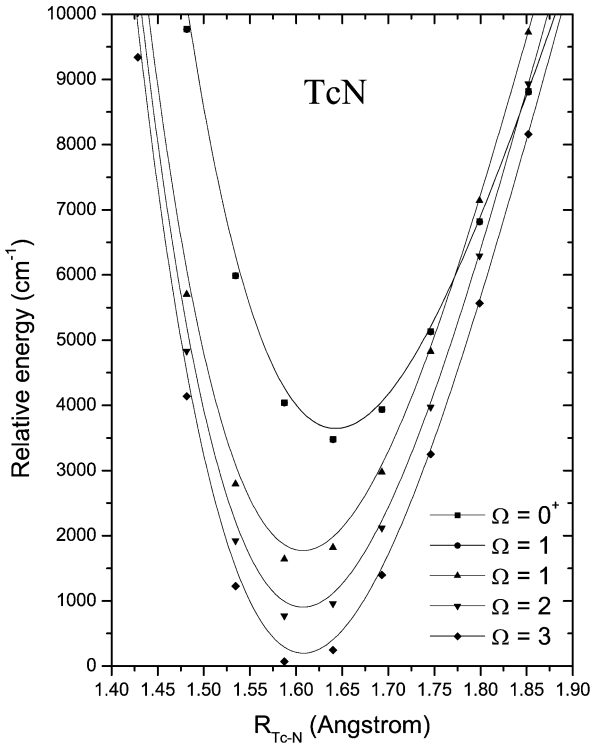

Figure 2. Potential energy curves for the lowest spin−orbit (Ω) states of TcN.

As for the TcN ground state, we start our discussion by considering a weak spin−orbit interaction and the possible candidates for the ground state of the other VIIB transition-metal monitrides. On the basis of this, we conclude that the ground state of TcN may be derived either from the $1\sigma^2 2\sigma^2 1\pi^4 1\delta^2 3\sigma^2$ or from the $1\sigma^2 2\sigma^2 1\pi^4 1\delta^2 3\sigma^1 2\pi^1$ electronic configuration (only valence orbitals were represented). Among the possible molecular electronic states, the singlets and those with $\Lambda \geq 3$ cannot correlate adiabatically with the two lowest energy dissociation asymptotic limits of the Tc and N atoms (Table 1). Besides that, neither configuration corresponds to the lowest-lying Λ−S molecular electronic state computed by us, a $^3\Delta$ state (Figure 1 and Table 2) correlating with the first excited atomic dissociation channel (Tc(^{6}D) + N($^4S^o$)). The $^3\Delta$ state can be derived from the electronic configuration $1\sigma^2 2\sigma^2 1\pi^4 1\delta^3 3\sigma^1$. It is worth recalling that of the VIIB transition metals, Tc is the one with the lowest $(n+1)s^2 nd^5(^6S) \rightarrow (n+1)s^1 nd^6(^6D)$ excitation energy, 0.41 eV (*J*-averaged value), against 2.14 and 1.71 eV for the Mn and Re atoms, respectively.[6] In contrast with the Mn atom, for which the ratio of the radial extent of the $(n+1)$s and *n*d atomic orbitals ($\langle(n+1)s|r|(n+1)s\rangle/\langle nd|r|nd\rangle = 2.99$) is very large,[40] for the Tc atom, the radial extents of the 4d and 5s atomic orbitals are more similar (2.27), which increases the possibility that the first atomic excited state of the Tc atom (Tc(^{6}D)) can take part in the formation of the ground state of the TcN molecule, as is the case for the $^3\Delta$ state.

In an energetic region below 6600 cm^{-1} (Figure 1 and Table 2), we have found four electronic states, with $^3\Delta$ being the lowest one. Next, there is a $^3\Sigma^-$ state, located (T_e) 2674 cm^{-1} higher in energy, and the $^5\Pi$ and $^1\Delta$ states, which are 6521 and 6576 cm^{-1} above the $^3\Delta$ state, respectively. The other electronic states are located in a higher energetic region ($\gtrsim$15 000 cm^{-1}).

Therefore, as long as a weak spin−orbit interaction is assumed, the TcN ground state is a $X^3\Delta$ state, which correlates with the first excited atomic dissociation channel (Tc(^{6}D) + N($^4S^o$)). Around the internuclear equilibrium distance (R_e = 1.605 Å), the wave function is dominated by a single configuration (87%)$|10\sigma^2 11\sigma^2 2\delta^3 12\sigma^1 5\pi^4\rangle$. The 10σ VMO is a nonbonding orbital corresponding to the N 2s atomic orbital; the 11σ VMO is a bonding orbital formed by the combination of the Tc $4d_\sigma$ and N $2p_\sigma$ atomic orbitals. The 12σ is a nonbonding VMO localized on the Tc atom, mainly described by the 5s atomic orbital with a minor contribution of $4d_\sigma$; the 13σ is an antibonding VMO formed by the linear combination of hybrid orbitals derived from the $4d_\sigma$ and 5s atomic orbitals of Tc and the 2s and $2p_\sigma$ orbitals of N. The 5π VMO is a bonding combination of the $4d_\pi$ (Tc) and $2p_\pi$ (N) atomic orbitals and the 6π VMO is the corresponding antibonding combination. Finally, the 2δ VMO is a nonbonding orbital composed of the

$4d_\delta$ Tc atomic orbitals. On the basis of this analysis, the chemical bonding in the ground state of the TcN molecule can be described by three normal two-electron bonds (11σ and 5π), two unpaired electrons localized on the transition-metal atom (2δ and 12σ), and one pair of isolated electrons on each atom (10σ on N and 2δ on Tc). The Mulliken population analysis (Tc/N: $5s^{0.87}5p_\sigma^{0.13}4d_\sigma^{1.05}4d_\delta^{2.98}4d_\pi^{1.72}/2s^{1.83}2p_\sigma^{1.10}2p_\pi^{2.17}$) (Table 3) corroborates these findings because the 5s and 2δ atomic orbitals are occupied by almost one electron, and the 2s atomic orbital is occupied by almost two; it also indicates a small charge transfer from Tc to the N atom, resulting in a dipole moment (μ) of 2.38 D ($Tc^{+0.16}N^{-0.16}$). The computed harmonic frequency (ω_e) is 1085 cm^{-1}, and the dissociation energy is 5.27 eV.

The definition of bond order, as presented above, is valid only when the wave function can be described by a single electron configuration. However, multiple bonds between transition-metal atoms can be described accurately only by the inclusion of configuration interaction. Configurations with fewer bonding and more antibonding electrons need to be taken into account to describe the particular contribution of each type of chemical bonding better. Therefore, a better definition of bond order can be obtained by considering the occupation numbers of bonding and antibonding natural orbitals derived from a multiconfigurational wave function, as defined by the EBO[41] analysis

$$\mathrm{EBO} = \sum \frac{(b_i - ab_i)}{2}$$

in which b_i and ab_i are, respectively, the natural occupation numbers of the bonding and corresponding antibonding natural orbitals. The EBO is, in general, a noninteger number, and the multiplicity of the chemical bonding is described by its next integer value. For the ground state of TcN, we have the following natural occupation numbers: $10\sigma^{1.99}11\sigma^{1.93}12\sigma^{1.00}13\sigma^{0.07}2\delta^{3.00}5\pi^{3.82}6\pi^{0.20}$. That is, the EBO is 2.74, corresponding to a triple bond, as obtained in the previous analysis. It is worth noting that the 10σ, 12σ, and 2δ VMOs, which are nonbonding VMOs centered on the atoms and do not play a significant role in the chemical bond, were not taken into account in computing the EBO.

The $A^3\Sigma^-$ electronic state, located (T_e) 2674 cm^{-1} above the $X^3\Delta$ state, with equilibrium internuclear distance of 1.640 Å and vibrational harmonic frequency of 1003 cm^{-1}, is the first excited electronic state of TcN. According to our results presented above, it would be the MnN ground state. Around its equilibrium internuclear distance, the $A^3\Sigma^-$ electronic wave function is dominated, at the CASSCF level, by the configuration $(83\%)|10\sigma^2 11\sigma^2 2\delta^2 12\sigma^2 5\pi^4\rangle$ (Table 3), derived from the $X^3\Delta$ state wave function by a single excitation ($2\delta \rightarrow 12\sigma$), involving nonbonding orbitals only. From the associated natural orbital occupation numbers, $10\sigma^{1.99}11\sigma^{1.93}12\sigma^{1.99}13\sigma^{0.08}2\delta^{2.00}5\pi^{3.76}6\pi^{0.24}$, the EBO is computed to be 2.68, indicating a triple bond. On the basis of the Mulliken population, (Tc/N) $5s^{1.53}5p_\sigma^{0.17}4d_\sigma^{1.22}4d_\delta^{2.00}4d_\pi^{1.90}/2s^{1.85}2p_\sigma^{1.20}2p_\pi^{2.00}$; in comparison with the $X^3\Delta$ state, there is a decrease in the population of the $4d_\delta$ orbital and an increase in the 5s orbital. There is only a small charge transfer from the metal to the main group element, as evidenced by the small magnitude of the dipole moment (μ = 0.25 D, $Tc^{+0.10}N^{-0.10}$). The $A^3\Sigma^-$ electronic state correlates adiabatically with the first atomic dissociation channel ($Tc(^6S) + N(^4S^o)$) (Table 1), with both atoms in the electronic ground state. The computed dissociation energy is 4.57 eV. It should be noted that, according to Balfour et al.[8,9] and Steimle et al.,[39] the ground state of ReN is a 0^+ state derived from a $^3\Sigma^-$ electronic state.

The second excited electronic state computed by us is the a $^5\Pi$ state (T_e = 6521 cm^{-1}, R_e = 1.670 Å, and ω_e = 947 cm^1), with a wave function dominated by a single configuration, $(83\%)|10\sigma^2 11\sigma^2 2\delta^2 12\sigma^1 5\pi^4 6\pi^1\rangle$ (Table 3), around the equilibrium internuclear distance; the $a^5\Pi$ state correlates adiabatically with the first excited atomic dissociation channel ($Tc(^6D) + N(^4S^o)$) (Table 1). In relation to the $X^3\Delta$ state, the $a^5\Pi$ is derived from a single excitation from the nonbonding 2δ VMO to the antibonding 6π VMO ($2\delta \rightarrow 6\pi$). The atomic orbital populations, given by (Tc/N) $5s^{0.89}5p_\sigma^{0.15}4d_\sigma^{1.07}4d_\delta^{2.00}4d_\pi^{2.45}/2s^{1.81}2p_\sigma^{1.06}2p_\pi^{2.41}$, indicate a reduction in the $4d_\delta$ orbital population and an increase in the $4d_\pi$ and $2p_\pi$ atomic orbitals and a great separation of charges ($Tc^{+0.51}N^{-0.51}$) resulting in a dipole moment of 2.77 D. The bonding VMO occupation numbers are $11\sigma^{1.91}5\pi^{3.81}$, with the remaining electrons distributed over nonbonding ($10\sigma^{1.99}12\sigma^{1.00}2\delta^{2.00}$) and antibonding ($13\sigma^{0.09}6\pi^{1.19}$) orbitals, resulting in an EBO of 2.22. The dissociation energy is computed to be 4.46 eV. In comparison with the other VIIB transition-metal monitrides, there is no mention of a $^5\Pi$ electronic state for ReN. However, as we have discussed above, our results indicate that there is a low-lying excited $^5\Pi$ in MnN, derived from the same electronic configuration as that for TcN ($|^5\Pi\rangle = (0.75)|7\sigma^2 8\sigma^2 9\sigma^1 3\pi^4 4\pi^1 1\delta^2\rangle$), located ($T_e$) 4193 cm^{-1} above our computed $X^3\Sigma^-$ state, with R_e = 1.606 Å, ω_e = 855 cm^{-1}, and μ = 2.85 D ($Mn^{\delta+}N^{\delta-}$). At the DFT level,[7,35] the $^5\Pi$ state would be the ground state of MnN.

At (T_e) 6576 cm^{-1} above the ground state and almost degenerate with the $a^5\Pi$, we computed the $b^1\Delta$ state, with an

TABLE 3: Wave Functions and Mulliken Populations of the Λ−S Electronic States of TcN

state	wave function	Mulliken population (Tc/N)
$X^3\Delta$	$(87\%)\|10\sigma^2 11\sigma^2 2\delta^3 12\sigma^1 5\pi^4\rangle$	$5s^{0.87}5p_\sigma^{0.13}4d_\sigma^{1.05}4d_\delta^{2.98}4d_\pi^{1.72}/2s^{1.83}2p_\sigma^{1.10}2p_\pi^{2.17}$
$A^3\Sigma^-$	$(83\%)\|10\sigma^2 11\sigma^2 2\delta^2 12\sigma^2 5\pi^4\rangle$	$5s^{1.53}5p_\sigma^{0.17}4d_\sigma^{1.22}4d_\delta^{2.00}4d_\pi^{1.90}/2s^{1.85}2p_\sigma^{1.20}2p_\pi^{2.00}$
$a^5\Pi$	$(83\%)\|10\sigma^2 11\sigma^2 2\delta^2 12\sigma^1 5\pi^4 6\pi^1\rangle$	$5s^{0.89}5p_\sigma^{0.15}4d_\sigma^{1.07}4d_\delta^{2.00}4d_\pi^{2.45}/2s^{1.81}2p_\sigma^{1.06}2p_\pi^{2.41}$
$b^1\Delta$	$(87\%)\|10\sigma^2 11\sigma^2 2\delta^3 12\sigma^1 5\pi^4\rangle$	$5s^{0.88}5p_\sigma^{0.22}4d_\sigma^{1.01}4d_\delta^{2.98}4d_\pi^{1.70}/2s^{1.84}2p_\sigma^{1.02}2p_\pi^{2.18}$
$B^3\Pi$	$(80\%)\|10\sigma^2 11\sigma^2 2\delta^2 12\sigma^1 5\pi^4 6\pi^1\rangle$	$5s^{0.88}5p_\sigma^{0.15}4d_\sigma^{1.01}4d_\delta^{2.02}4d_\pi^{2.60}/2s^{1.83}2p_\sigma^{1.09}2p_\pi^{2.30}$
$C^3\Pi$	$(80\%)\|10\sigma^2 11\sigma^2 2\delta^2 12\sigma^1 5\pi^4 6\pi^1\rangle$	$5s^{0.91}5p_\sigma^{0.15}4d_\sigma^{1.07}4d_\delta^{2.01}4d_\pi^{2.51}/2s^{1.83}2p_\sigma^{1.02}2p_\pi^{2.38}$
$c^5\Sigma^-$	$(74\%)\|10\sigma^2 11\sigma^2 2\delta^2 12\sigma^2 5\pi^3 6\pi^1\rangle$	$5s^{1.38}5p_\sigma^{0.06}4d_\sigma^{1.30}4d_\delta^{2.00}4d_\pi^{2.00}/2s^{1.89}2p_\sigma^{1.34}2p_\pi^{1.96}$
$d^5\Delta$	$(80\%)\|10\sigma^2 11\sigma^2 2\delta^3 12\sigma^1 5\pi^3 6\pi^1\rangle$	$5s^{0.84}5p_\sigma^{0.06}4d_\sigma^{0.91}4d_\delta^{2.98}4d_\pi^{1.89}/2s^{1.87}2p_\sigma^{1.30}2p_\pi^{2.06}$
$e^7\Pi$	$(73\%)\|10\sigma^2 11\sigma^2 2\delta^2 12\sigma^1 5\pi^3 6\pi^2\rangle$	$5s^{0.89}5p_\sigma^{0.18}4d_\sigma^{1.03}4d_\delta^{2.00}4d_\pi^{2.31}/2s^{1.87}2p_\sigma^{1.01}2p_\pi^{2.55}$
$f^7\Sigma^-$	$(92\%)\|10\sigma^2 11\sigma^1 2\delta^2 12\sigma^1 5\pi^4 6\pi^2\rangle$	$5s^{0.82}5p_\sigma^{0.06}4d_\sigma^{0.69}4d_\delta^{2.00}4d_\pi^{2.84}/2s^{1.76}2p_\sigma^{0.66}2p_\pi^{2.94}$
$g^9\Sigma^-$	$(58\%)\|10\sigma^2 11\sigma^2 2\delta^2 12\sigma^1 13\sigma^1 5\pi^2 6\pi^2\rangle$ $(42\%)\|10\sigma^2 11\sigma^1 2\delta^2 12\sigma^2 13\sigma^1 5\pi^2 6\pi^2\rangle$	$5s^{1.00}5p_\sigma^{0.12}4d_\sigma^{1.60}4d_\delta^{2.00}4d_\pi^{2.00}/2s^{1.95}2p_\sigma^{1.31}2p_\pi^{1.98}$
$h^7\Pi$	$(60\%)\|10\sigma^2 11\sigma^1 2\delta^2 12\sigma^1 13\sigma^1 5\pi^4 6\pi^1\rangle$ $(14\%)\|10\sigma^2 11\sigma^2 2\delta^2 12\sigma^1 5\pi^3 6\pi^2\rangle$	$5s^{0.89}5p_\sigma^{0.27}4d_\sigma^{0.98}4d_\delta^{2.01}4d_\pi^{2.29}/2s^{1.83}2p_\sigma^{1.00}2p_\pi^{2.58}$
$i^9\Pi$	$(100\%)\|10\sigma^2 11\sigma^1 2\delta^2 12\sigma^1 13\sigma^1 5\pi^3 6\pi^2\rangle$	$5s^{0.90}5p_\sigma^{0.30}4d_\sigma^{0.99}4d_\delta^{2.00}4d_\pi^{2.01}/2s^{1.88}2p_\sigma^{0.92}2p_\pi^{2.78}$

TABLE 4: Theoretical Spectroscopic Constants for the Spin−Orbit (Ω) States of TcN

Ω	R_e (Å)	ω_e (cm^{-1})	T_e (cm^{-1})	G_0 (cm^{-1})	$\Delta G_{1/2}$ (cm^{-1})
(1)3	1.605	1085	0	540	1073
(2)2	1.605	1088	704	542	1075
(3)1	1.605	1085	1574	540	1073
(4)1	1.640	1000	3475	499	988
(5)0^+	1.640	1000	3477	499	988

equilibrium internuclear distance of 1.591 Å and harmonic vibrational frequency of 1131 cm^{-1}. In the equilibrium internuclear region, the $b^1\Delta$ wave function is dominated by a single electronic configuration, $(87\%)|10\sigma^2 11\sigma^2 2\delta^3 12\sigma^1 5\pi^4\rangle$ (Table 3). The $b^1\Delta$ state correlates adiabatically with a higher excited atomic dissociation channel. The Mulliken population analysis is $5s^{0.88}5p_\sigma^{0.22}4d_\sigma^{1.01}4d_\delta^{2.98}4d_\pi^{1.70}/2s^{1.84}2p_\sigma^{1.02}2p_\pi^{2.18}$, corresponding to a dipole moment of 0.20 D and +0.10e on Tc. From the corresponding natural orbital occupation numbers ($10\sigma^{1.99}11\sigma^{1.93}12\sigma^{1.00}13\sigma^{0.07}2\delta^{2.00}5\pi^{3.83}6\pi^{0.18}$), an EBO of 2.75 is computed.

3.2. Low-Lying Ω States of TcN. The $^3\Delta$, $^3\Sigma^-$, $^5\Pi$, and $^1\Delta$ Λ−S electronic states are well separated from the others (Figure 1 and Table 2). Although spin−orbit coupling mixes different Λ−S electronic states, the greater the energy difference between them, the lesser will be the influence of the spin−orbit coupling with the ground state. Therefore, rather than include all states in the treatment of the spin−orbit coupling, for the description of the ground state, we took into account only those spin−orbit states derived from the four Λ−S electronic states mentioned above. When the spin−orbit coupling is taken into account, the four lowest-lying Λ−S electronic states of TcN ($^3\Delta$, $^3\Sigma^-$, $^5\Pi$, and $^1\Delta$) lead to the following Ω states (number of states in parentheses):[34,33,42] 0^+(2), 0^-(1), 1(4), 2(3), and 3(2). The energies and spectroscopic constants for the lowest spin−orbit states considered in this contribution are displayed in Table 4.

The $X^3\Delta$ Λ−S electronic state gives rise to the three lowest-lying Ω states (Ω = 3, 2, 1). The lowest one is the (1)3 (Table 4), with an equilibrium internuclear distance of 1.605 Å and ω_e = 1085 cm^{-1}. As we have pointed out, the $X^3\Delta$ state correlates adiabatically to the first excited atomic dissociation channel (Tc(^{6}D) + N(^{4}S^o)) (Table 1). From the corresponding atomic spectroscopic terms, Tc(^{6}D) + N(^{4}S^o), the following molecular spin−orbit states arise (number of states in parentheses):[34,33] 4, 3(2), 2(3), 1(4), $0^\pm$(2).

The next Ω state derived from the $X^3\Delta$ state is the (2)2 state, placed (T_e) 704 cm^{-1} above the (1)3 state, with equilibrium internuclear distance of 1.605 Å and ω_e = 1088 cm^{-1} (Figure 2 and Table 4). Next, we found the (3)1 state, the lower Ω = 1 state (the last Ω state derived from the $X^3\Delta$ state), located 1574 cm^{-1} higher in energy (T_e) than the low-lying (1)3 state, with R_e = 1.605 Å and ω_e = 1085 cm^{-1}.

The Ω states (4)1 and (5)0^+ are derived from the $A^3\Sigma^-$ Λ−S state. The (4)1 and (5)0^+ spin−orbit states are very close in energy (T_e = 3475 and 3477 cm^{-1}, respectively), with the same internuclear equilibrium distance (1.640 Å) and vibrational harmonic frequency (1000 cm^{-1}). It is worth mentioning that because off-diagonal interactions were not included the (4)1−(5)0^+ splitting may be larger than was predicted in this work. The $A^3\Sigma^-$ electronic state correlates adiabatically with the first atomic dissociation channel (Tc(^{6}S) + N(^{4}S^o)) (Table 1), with both atoms in the electronic ground state. After taking into account the spin−orbit interaction between the asymptotic atomic states, the following molecular spin−orbit states arise (number of states in parentheses):[34,33] 4, 3(2), 2(3), 1(4), $0^\pm$(2).

In comparison with the ReN molecule, we note a difference in relation to the predicted ground electronic state. Balfour et al.[8,9] and Steimle et al.,[39] on the basis of experimental results, proposed a Ω = 0^+ state, derived from a $X^3\Sigma^-$ Λ−S state as the ReN ground state. For TcN, however, our theoretical results point to a Ω = 3 ground state, being mainly of $X^3\Delta$ character.

3.3. Higher Λ−S Electronic States of TcN. The next two triplet electronic states are the $B^3\Pi$ and $C^3\Pi$ states (Figure 1 and Table 2). At (T_e) 15 753 cm^{-1} above the ground state, the $B^3\Pi$ electronic state (R_e = 1.697 Å, ω_e = 854 cm^{-1}, and μ = 2.06 D) is found, with a wave function best described by a single electronic configuration, $(80\%)|10\sigma^2 11\sigma^2 2\delta^2 12\sigma^1 5\pi^4 6\pi^1\rangle$ (Table 3), around the equilibrium internuclear region. In comparison with the ground state, the $B^3\Pi$ state is obtained by a single excitation ($2\delta \rightarrow 6\pi$), representing a charge transfer from the 2δ nonbonding VMO to the antibonding 6π VMO. The Mulliken population analysis is given as Tc/N: $5s^{0.88}5p_\sigma^{0.15}4d_\sigma^{1.01}$-$4d_\delta^{2.02}4d_\pi^{2.60}/2s^{1.83}2p_\sigma^{1.09}2p_\pi^{2.30}$. From the valence natural orbital occupation numbers ($10\sigma^{1.99}11\sigma^{1.90}12\sigma^{0.98}13\sigma^{0.09}2\delta^{2.03}5\pi^{3.80}6\pi^{1.20}$), the EBO for the $B^3\Pi$ state is 2.21. The $C^3\Pi$ state is placed 16 998 cm^{-1} above the ground state, with R_e = 1.671 Å, ω_e = 965 cm^{-1}, and a wave function dominated by the single configuration $(80\%)|10\sigma^2 11\sigma^2 2\delta^2 12\sigma^1 5\pi^4 6\pi^1\rangle$, derived from the ground state by a single excitation ($2\delta \rightarrow 6\pi$). The Mulliken population is (Tc/N) $5s^{0.91}5p_\sigma^{0.15}4d_\sigma^{1.07}4d_\delta^{2.01}4d_\pi^{2.51}/2s^{1.83}2p_\sigma^{1.02}2p_\pi^{2.38}$, and the natural orbital population analysis is given by $10\sigma^{1.99}11\sigma^{1.90}12\sigma^{0.88}13\sigma^{0.09}2\delta^{2.13}5\pi^{3.81}6\pi^{1.18}$, resulting in EBO = 2.22 and μ = 2.02 D.

The next two excited states are the $c^5\Sigma^-$ and the $d^5\Delta$ states (Figure 1 and Table 2), located (T_e) 22 140 and 23 880 cm^{-1} above the ground state, respectively. Around its equilibrium internuclear distance (R_e = 1.888 Å and ω_e = 663 cm^{-1}), the wave function for the $c^5\Sigma^-$ state is best described by the $(74\%)|10\sigma^2 11\sigma^2 2\delta^2 12\sigma^2 5\pi^3 6\pi^1\rangle$ electronic configuration, derived from the ground state by a double excitation (2δ, $5\pi \rightarrow 12\sigma$, 6π), increasing the population of the σ,π-system and decreasing the population of the δ orbitals. The Mulliken population analysis and the natural orbital occupation numbers are given as ($5s^{1.38}5p_\sigma^{0.06}4d_\sigma^{1.30}4d_\delta^{2.00}4d_\pi^{2.00}/2s^{1.89}2p_\sigma^{1.34}2p_\pi^{1.96}$) and ($10\sigma^{2.00}11\sigma^{1.90}12\sigma^{1.98}13\sigma^{0.11}2\delta^{2.00}5\pi^{2.70}6\pi^{1.24}$), respectively, with a dipole moment of 1.53 D and EBO of 1.63. The $d^5\Delta$ state (T_e = 23 880 cm^{-1}, R_e = 1.850 Å, and ω_e = 710 cm^{-1}) wave function is dominated by the configuration $(80\%)|10\sigma^2 11\sigma^2 2\delta^3 12\sigma^1 5\pi^3 6\pi^1\rangle$, derived from the ground state by a single excitation from a bonding to an antibonding orbital ($5\pi \rightarrow 6\pi$). The Mulliken population analysis is (Tc/N) $5s^{0.84}5p_\sigma^{0.06}4d_\sigma^{0.91}4d_\delta^{2.98}$ $4d_\pi^{1.89}/2s^{1.87}2p_\sigma^{1.30}2p_\pi^{2.06}$, and the natural orbital occupation numbers are $10\sigma^{2.00}11\sigma^{1.89}12\sigma^{1.01}13\sigma^{0.11}2\delta^{2.99}5\pi^{2.80}6\pi^{1.22}$, with μ = 2.80 D and EBO of 1.68.

Following the quintet states, we have computed two heptet and two nonet excited states located greater than 25 000 cm^{-1} above the ground state. A double excitation from a bonding (5π) and a nonbonding (2δ) to antibonding VMOs (6π) gives rise to the $e^7\Pi$ state (R_e = 1.884 Å and ω_e = 726 cm^{-1}). Placed at 25 044 cm^{-1} above the ground state, its wave function is dominated by the $(73\%)|10\sigma^2 11\sigma^2 2\delta^2 12\sigma^1 5\pi^3 6\pi^2\rangle$ electronic configuration (Tables 2 and 3), with the following Mulliken population: $5s^{0.89}5p_\sigma^{0.18}4d_\sigma^{1.03}4d_\delta^{2.00}4d_\pi^{2.31}/2s^{1.87}2p_\sigma^{1.01}2p_\pi^{2.55}$, with a dipole moment of 2.40 D. The natural orbital occupation numbers, $10\sigma^{2.00}11\sigma^{1.69}12\sigma^{1.00}13\sigma^{0.30}2\delta^{3.00}5\pi^{3.03}6\pi^{1.97}$, result in an EBO of 1.23. At 28 858 cm^{-1} (T_e), is the $f^7\Sigma^-$ electronic state, with R_e = 1.815 Å and ω_e = 755 cm^{-1}. Its wave function is described best by the $(92\%)|10\sigma^2 11\sigma^1 2\delta^2 12\sigma^1 5\pi^4 6\pi^2\rangle$ electronic configuration, which differs from that for the X state by a double excitation (11σ, $2\delta \rightarrow 6\pi$). The Mulliken population analysis (Tc/N) is given by $5s^{0.82}5p_\sigma^{0.06}4d_\sigma^{0.69}4d_\delta^{2.00}4d_\pi^{2.84}$/

$2s^{1.76}2p_{\sigma}^{0.66}2p_{\pi}^{2.94}$, which reflects the increase in the population of electrons in the π-system and a decrease in the σ,δ-system; the dipole moment is computed to be 3.26 D. An EBO of 1.35 can be derived from the following natural orbital occupation numbers: $10\sigma^{1.99}11\sigma^{0.97}12\sigma^{1.00}13\sigma^{0.06}2\delta^{2.00}5\pi^{3.88}6\pi^{2.10}$.

The first nonet state, $g^9\Sigma^-$, is located 37 570 cm^{-1} higher in energy than the ground state, with $R_e = 2.144$ Å, $\omega_e = 630$ cm^{-1}, and $\mu = 0.39$ D. Its wave function is better described by the combination of two electronic configurations, $(58\%)|10\sigma^2 11\sigma^2 2\delta^2 12\sigma^1 13\sigma^1 5\pi^2 6\pi^2\rangle + (42\%)|10\sigma^2 11\sigma^1 2\delta^2 12\sigma^2 13\sigma^1 5\pi^2 6\pi^2\rangle$, which correspond to triple excitations ($2\delta, 5\pi \rightarrow 13\sigma, 6\pi$ and $11\sigma, 5\pi \rightarrow 13\sigma, 6\pi$) with respect to the ground state. The associated Mulliken population analysis is $5s^{1.00}5p_{\sigma}^{0.12}4d_{\sigma}^{1.60}4d_{\delta}^{2.00}4d_{\pi}^{2.00}/2s^{1.95}2p_{\sigma}^{1.31}2p_{\pi}^{1.98}$, whereas the natural orbital occupation numbers are: $10\sigma^{2.00}11\sigma^{1.00}12\sigma^{1.00}13\sigma^{1.00}2\delta^{2.00}5\pi^{3.00}6\pi^{2.00}$; the EBO is 1.00. The $i^9\Pi$ state ($T_e = 41\,721$ cm^{-1}, $R_e = 2.130$ Å, $\mu = 2.18$ D, and $\omega_e = 537$ cm^{-1}) is the other nonet included in this work. Its wave function is dominated by a single configuration $|10\sigma^2 11\sigma^1 2\delta^2 12\sigma^1 13\sigma^1 5\pi^3 6\pi^2\rangle$ corresponding to triple excitations ($11\sigma, 2\delta, 5\pi \rightarrow 13\sigma, 6\pi$). The Mulliken population is given by $5s^{0.90}5p_{\sigma}^{0.30}4d_{\sigma}^{0.99}4d_{\delta}^{2.00}4d_{\pi}^{2.01}/2s^{1.88}2p_{\sigma}^{0.92}2p_{\pi}^{2.78}$, and the natural orbital occupation numbers are $10\sigma^{2.00}11\sigma^{1.00}12\sigma^{1.00}13\sigma^{1.00}2\delta^{2.00}5\pi^{2.00}6\pi^{1.00}$, resulting in an EBO of 1.00.

Between the $g^9\Sigma^-$ and the $i^9\Pi$ states, we found the $h^7\Pi$ state ($T_e = 38489$ cm^{-1}, $R_e = 1.901$ Å, $\omega_e = 622$ cm^{-1}, and $\mu = 1.44$ D). Around its equilibrium internuclear distance, the $h^7\Pi$ wave function is best described as $(60\%)|10\sigma^2 11\sigma^1 2\delta^2 12\sigma^1 13\sigma^1 5\pi^4 6\pi^1\rangle + (14\%)|10\sigma^2 11\sigma^2 2\delta^2 12\sigma^1 5\pi^3 6\pi^2\rangle$, involving at least two electronic configurations. The Mulliken population analysis is given as $5s^{0.89}5p_{\sigma}^{0.27}4d_{\sigma}^{0.98}4d_{\delta}^{2.01}4d_{\pi}^{2.29}/2s^{1.83}2p_{\sigma}^{1.00}2p_{\pi}^{2.58}$, and the natural occupation numbers, $10\sigma^{2.00}11\sigma^{2.00}12\sigma^{1.00}13\sigma^{1.00}2\delta^{2.00}5\pi^{1.00}6\pi^{1.00}$, result in EBO = 1.0.

4. Conclusions

The lowest-lying $X^3\Delta$, $A^3\Sigma^-$, $a^5\Pi$, $b^1\Delta$, $B^3\Pi$, $C^3\Pi$, $c^5\Sigma^-$, $d^5\Delta$, $e^7\Pi$, $f^7\Sigma^-$, $g^9\Sigma^-$, $h^7\Pi$, and $i^9\Pi$ electronic states of TcN have been investigated at the ab initio CASPT2 level with an extended atomic basis set and the inclusion of scalar relativistic effects. Spin−orbit calculations were performed for the $X^3\Delta$, $A^3\Sigma^-$, $a^5\Pi$, and $b^1\Delta$ Λ−S states. Potential energy curves, spectroscopic constants, dipole moments, and EBO have been reported for all states. The TcN ground state was computed to be of $^3\Delta$ symmetry, with equilibrium internuclear distance of 1.605 Å, $\omega_e = 1085$ cm^{-1}, $D_e = 5.27$ eV, and EBO equal to 2.74, indicating a triple bond between the atoms. After the inclusion of the spin−orbit interaction, the ground state turns out to be the $\Omega = 3$ state of $^3\Delta$ character, with $R_e = 1.605$ Å and $\omega_e = 1085$ cm^{-1}.

Acknowledgment. J.P.G. is grateful to FAPESP (Fundação de Amparo à Pesquisa do Estado de São Paulo, Brazil) for a graduate fellowship. A.C.B. acknowledges CNPq (Conselho Nacional de Desenvolvimento Científico e Tecnológico, Brazil) and FAPESP.

References and Notes

(1) Harrison, J. F. *Chem. Rev.* **2000**, *100*, 679.
(2) Sahu, B. R.; Kleinman, L. *Phys. Rev. B* **2003**, *68*, 113101.
(3) Lambrecht, W. R. L.; Prikhodko, M.; Miao, M. S. *Phys. Rev. B* **2003**, *68*, 174411.
(4) Marques, M.; Teles, L. K.; Scolfaro, L. M. R.; Furthmüller, J.; Bechstedt, F.; Ferreira, L. G. *Appl. Phys. Lett.* **2005**, *86*, 164105.
(5) Marques, M.; Scolfaro, L. M. R.; Teles, L. K.; Furthmüller, J.; Bechstedt, F.; Ferreira, L. G. *Appl. Phys. Lett.* **2006**, *88*, 022507.
(6) Sansonetti, J.; Martin, W.; Young, S. *Handbook of Basic Atomic Spectroscopic Data*, version 1.00; National Institute of Standards and Technology: Gaithersburg, MD, 2003. http://physics.nist.gov/Handbook.
(7) Andrews, L.; Bare, W. D.; Chertihin, G. V. *J. Phys. Chem. A* **1997**, *101*, 8417.
(8) Balfour, W. J.; Cao, J.; Qian, C. X. W.; Rixon, S. J. *J. Mol. Spectrosc.* **1997**, *183*, 113.
(9) Cao, J.; Balfour, W. J.; Qian, C. X. W. *J. Phys. Chem. A* **1997**, *101*, 6741.
(10) Jackson, P.; Gadd, G. E.; Mackey, D. W.; van der Wall, H.; Willett, G. D. *J. Phys. Chem. A* **1998**, *102*, 8941.
(11) Langhoff, S. R.; Bauschlicher; Jr, C. W.; Pettersson, L. G. M.; Siegbahn, P. E. M. *Chem. Phys.* **1989**, *132*, 49.
(12) Bauschlicher, C. W.; Langhoff, S. R.; Partridge, H. In *Modern Electronic Structure Theory, Part II*; Yarkony, D. R., Ed.; World Scientific: London, 1995; p 1280.
(13) Siegbahn, P. E. M. In *Adv. Chem. Phys.*; Prigogine, I., Rice, S. A., Eds.; John Wiley & Sons: Chichester, England, 1996; p 333.
(14) Frenking, G.; Fröhlich, N. *Chem. Rev.* **2000**, *100*, 679.
(15) Roos, B. O. In *Advances in Chemical Physics: Ab Initio Methods in Quantum Chemistry II*; Lawley, K. P., Ed.; John Wiley & Sons: Chichester, 1987; p 399.
(16) Andersson, K.; Malmqvist, P.-Å.; Roos, B. O.; Sadlej, A. J.; Wolinski, K. *J. Phys. Chem.* **1990**, *94*, 5483.
(17) Andersson, K.; Malmqvist, P.-Å.; Roos, B. O. *J. Chem. Phys.* **1992**, *96*, 1218.
(18) Roos, B. O.; Andersson, K.; Fülscher, M. P.; Malmqvist, P.-Å.; Serrano-Andrés, L.; Pierloot, K.; Merchán, M. In *Advances in Chemical Physics: New Methods in Computational Quantum Mechanics*; Prigogine, I., Rice, S. A., Eds.; John Wiley & Sons: New York, 1996; p 219.
(19) Borin, A. C.; Gobbo, J. P.; Roos, B. O. *Chem. Phys. Lett.* **2006**, *418*, 311.
(20) Gobbo, J. P.; Borin, A. C. *J. Chem. Phys.* **2007**, *126*, 011102.
(21) Borin, A. C.; Gobbo, J. P. *J. Phys. Chem. A* **2008**, *112*, 4394.
(22) Borin, A. C.; Gobbo, J. P.; Roos, B. O. *Chem. Phys.* **2008**, *343*, 210.
(23) Borin, A. C.; Gobbo, J. P.; Roos, B. O. *Mol. Phys.* **2009**, *107*, 1035.
(24) Douglas, M.; Kroll, N. M. *Ann. Phys.* **1974**, *82*, 89.
(25) Hess, B. A. *Phys. Rev.* **1986**, *33*, 3742.
(26) Roos, B. O.; Lindh, R.; Malmqvist, P.-Å.; Veryazov, V.; Widmark, P. O *J. Phys. Chem. A* **2005**, *109*, 6575.
(27) Widmark, P.; Malmqvist, P.-Å.; Roos, B. O. *Theor. Chim. Acta.* **1990**, *77*, 291.
(28) Ghigo, G.; Roos, B. O.; Malmqvist, P.-Å. *Chem. Phys. Lett.* **2004**, *396*, 142.
(29) Hess, B. A.; Marian, C. M.; Wahlgren, U.; Gropen, O. *Chem. Phys. Lett.* **1996**, *251*, 365.
(30) Roos, B. O.; Malmqvist, P.-Å. *Phys. Chem. Chem. Phys.* **2004**, *6*, 2919.
(31) Malmqvist, P.-Å.; Roos, B. O.; Schimmelpfenning, B. *Chem. Phys. Lett.* **2002**, *357*, 230.
(32) Karlström, G.; Lindh, R.; Malmqvist, P.-Å.; Roos, B. O.; Ryde, U.; Veryazov, V.; Widmark, P.-O.; Cossi, M.; Schimmelpfennig, B.; Neogrady, P.; Seijo, L. *Comput. Mater. Sci.* **2003**, *28*, 222.
(33) Lefebvre-Brion, H.; Field, R. W. *The Spectra and Dynamics of Diatomic Molecules*; Elsevier: Boston, 2004.
(34) Herzberg, G. *Molecular Spectra and Molecular Structure: Spectra of Diatomic Molecules*; Van Nostrand Reinhold: New York, 1950; Vol. 1H.
(35) Wu, Z. *J. Comput. Chem.* **2006**, *27*, 267.
(36) Barden, C. J.; Rienstra-Kiracofe, J. C.; Schaefer, H. F., III. *J. Chem. Phys.* **2000**, *113*, 690.
(37) Gobbo, J. P.; Borin, A. C. *J. Phys. Chem. A* **2006**, *110*, 13966.
(38) Cernusák, I.; Dallos, M.; Lischka, H.; Müller, T.; Uhlár, M. *J. Chem. Phys.* **2007**, *126*, 214311.
(39) Steimle, T. C.; Virgo, W. L. *J. Chem. Phys.* **2004**, *121*, 124111.
(40) Rakowitz, F.; Marian, C. M.; Seijo, L.; Wahlgren, U. *J. Chem. Phys.* **1999**, *110*, 3678.
(41) Roos, B. O.; Borin, A. C.; Gagliardi, L. *Angew. Chem., Int. Ed.* **2007**, *46*, 1469.
(42) Balasubramanian, K. *Relativistic Effects in Chemistry, Part A*; John Wiley and Sons, Inc.: New York, 1997.

JP902545H